The Journal of Neuroscience, September 1, 2001, *21*(17):6732–6744

α4 Integrin Is Expressed during Peripheral Nerve Regeneration and Enhances Neurite Outgrowth

Mariette G. Vogelezang,[1] ZhiQiang Liu,[2] João B. Relvas,[1] Gennadij Raivich,[2] Steven S. Scherer,[3] and Charles ffrench-Constant[1]

[1]Department of Medical Genetics, University of Cambridge and Cambridge Centre for Brain Repair, University Forvie Site, Cambridge, CB2 2PY, United Kingdom, [2]Department of Neuromorphology, Max Planck Institute for Neurobiology, D-82152 Martinsried, Germany, and [3]Department of Neurology, The University of Pennsylvania Medical Center, Philadelphia, Pennsylvania 19104

We have shown previously that repair in the peripheral nervous system is associated with a reversion to an embryonic pattern of alternative splicing of the extracellular matrix molecule fibronectin. One of the consequent changes is a relative increase in the number of fibronectins expressing the binding site for α4 integrins. Here we show that α4 integrins are expressed on dorsal root ganglion neuron cell bodies and growth cones in the sciatic nerve during regeneration and that the interaction of α4 integrin with alternatively spliced isoforms of recombinant fibronectins containing the α4 binding site enhances neurite outgrowth in dorsal root ganglion neurons. The pheochromocytoma (PC12) neuronal cell line, which normally extends neurites poorly on fibronectin, does so efficiently when α4 is expressed in the cells. Experiments using chimeric integrins expressed in PC12 cells show that the α4 cytoplasmic domain is necessary and sufficient for this enhanced neurite outgrowth. In both dorsal root ganglion neurons and PC12 cells the α4 cytoplasmic domain is tightly linked to the intracellular adapter protein paxillin. These experiments suggest an important role for α4 integrin and paxillin in peripheral nerve regeneration and show how alternative splicing of fibronectin may provide a mechanism to enhance repair after injury.

Key words: integrin; peripheral nerve regeneration; fibronectin; alternative splicing; paxillin; α4; PC12 cell; dorsal root ganglia; chimera; LDV

Damage to the peripheral nervous system (PNS) is followed by Wallerian degeneration of axons distal to the lesion site associated with increased expression of extracellular matrix (ECM) molecules including fibronectin (FN) (Lefcort et al., 1992; Martini, 1994; Scherer and Salzer, 1996). Antibody-blocking experiments suggest that these increased levels of FN contribute to the subsequent repair (Toyota et al., 1990; Wang et al., 1992; Bailey et al., 1993; Agius and Cochard, 1998). FN is expressed as different isoforms generated by alternative splicing of the primary gene transcript. Two type III repeats EIIIA and EIIIB are either included or excluded, whereas the V (IIICS) region can be partly or completely excluded in patterns that differ between species (Schwarzbauer et al., 1983, 1987; Tamkun et al., 1984; Kornblihtt et al., 1985; Gutman and Kornblihtt, 1987; Zardi et al., 1987). In the rat, three different forms (V0, V95, and V120) can be generated (Fig. 1). The latter two differ by the inclusion or exclusion of the first 25 amino acids, a segment called V25. This segment contains a cell-binding sequence Leu-Asp-Val (LDV) that is recognized by the integrins α4β1 and α4β7 (Wayner et al., 1989; Guan and Hynes, 1990). This cell-binding site is distinct from the Arg-Gly-Asp (RGD) sequence within the 10[th] type III repeat (Fig. 1), recognized by other integrins including α5β1 (Ruoslahti, 1996). The expression of the alternatively spliced isoforms of FN *in vivo* is developmentally regulated. Most FN mRNA early in development is EIIIA+, EIIIB+, and V+, whereas in the adult these exons are excluded in a cell- and tissue-specific pattern (Magnuson et al., 1991; ffrench-Constant, 1995; Peters and Hynes, 1996; Peters et al., 1996).

The regulation of splicing suggests that the alternatively spliced isoforms of FN possess unique properties. In light of this, we previously examined the pattern of FN splicing during sciatic nerve regeneration in the rat. We observed an increase in the relative percentage of EIIIA+, EIIIB+, and V25+ forms of FN in the nerve (Mathews and ffrench-Constant, 1995; Vogelezang et al., 1999), as also described in other models of injury and disease (for review, see ffrench-Constant, 1995). The relative increase of the α4 integrin binding site within V25 (from 19% of total FN mRNA to 29–38%, becoming the most abundant V isoform) was of particular interest. Previous work has shown distinct roles for the α4 and α5 integrins in neural crest cell migration (Dufour et al., 1988; Kil et al., 1998) and dorsal root ganglion (DRG) neurite outgrowth (Humphries et al., 1988). We therefore proposed a model in which increased expression of V25 would enhance neurite outgrowth by simultaneous presentation of the α4β1 and α5β1 cell-binding sites to the regrowing axon. The goals of this study were twofold: first, to test the predictions from this model that α4 integrins would be expressed on regenerating growth cones in the adult nerve and would activate intracellular signaling

Received Feb. 1, 2001; revised May 18, 2001; accepted May 31, 2001.

This work was supported by Action Research (Horsham, UK) (M.G.V., C.ff.-C.), a fellowship (BPD 11785) from the Programa Praxis XXI of the Fundacão para a Ciência é Tecnologia (Portugal) (J.B.R.), and by Deutsche Forschungsgemeinschaft RA486/3–2 and RA486/8–2 (G.R.). We are extremely grateful to Monique Jouet and Andreas Faissner for help with the production of the recombinant fibronectins and Dr. Paul Mould for advice concerning the LAV mutations.

Correspondence should be addressed to Dr. Charles ffrench-Constant, Department of Medical Genetics, University of Cambridge and Cambridge Centre for Brain Repair, University Forvie Site, Robinson Way, Cambridge, CB2 2PY, UK. E-mail: cfc@mole.bio.cam.ac.uk.

G. Raivich's present address: Department of Obstetrics and Gynecology and Department of Anatomy, University College London, Gower Street, London WC2, UK.

Copyright © 2001 Society for Neuroscience 0270-6474/01/216732-13$15.00/0

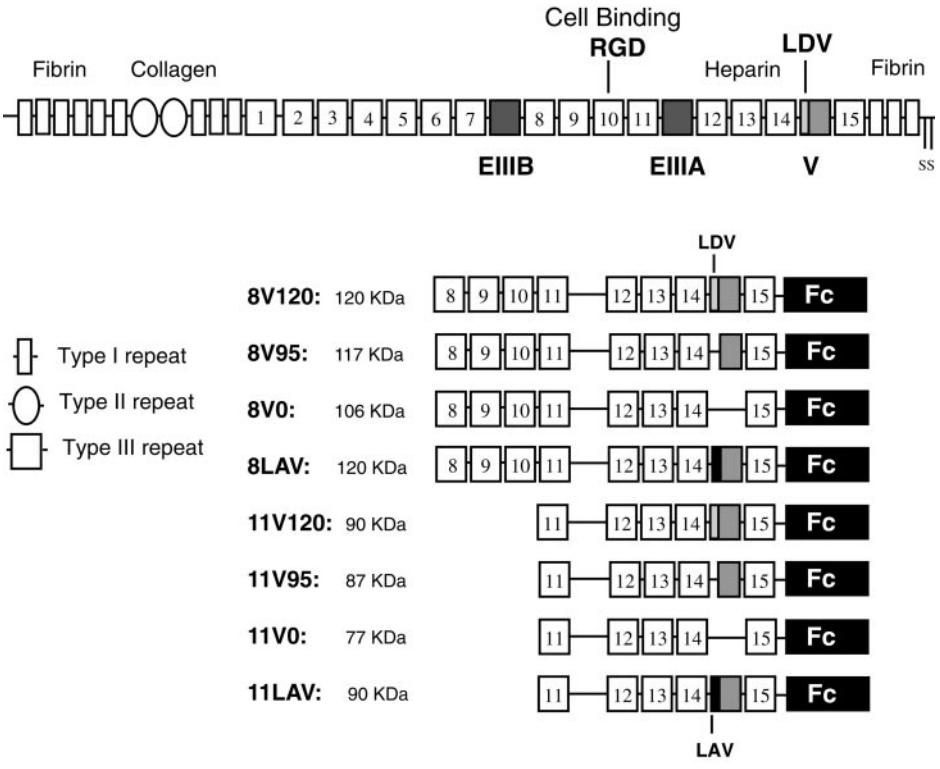

Figure 1. Schematic drawing of rat FN and the recombinant fragments made in this study. *Shaded boxes* mark the three alternatively spliced regions in FN. Each of the recombinant fragments used is illustrated, and the approximate molecular size shown. The $\alpha5\beta1$ recognition sequence, Arg-Gly-Asp (*RGD*) is located in the 10th type III repeat. The $\alpha4\beta1$ binding sequence Leu-Asp-Val (*LDV*) is located in the V25 fragment. Note the pattern of V region splicing, as described in the introductory remarks, shown in the two sets of recombinant FNs: 8V120 and 11V120, V95, and V0. The V120 form contains a 25 amino acid sequence (V25) that includes the LDV sequence to which $\alpha4\beta1$ binds. This is shown as a *light gray box*. In those recombinant FNs in which this sequence was mutated to LAV (to abolish $\alpha4\beta1$ binding), the V25 region is shown as a *black box*. Construction of the recombinant fragments is described in Materials and Methods. All fragments carry at their C termini the 232 amino acid sequence of the human IgG_1 Fc that is represented by the *filled rectangles*.

pathways leading to enhanced neuronal growth; second, to begin to identify the initial components of the intracellular signaling pathway involved.

MATERIALS AND METHODS

Antibodies. The following antibodies were used: mouse anti-rat α4, clone MR 4–1 (PharMingen, San Diego, CA); rat anti-mouse α4, clone R1-2 (PharMingen); mouse anti-human α4, clone HP2/1 (Chemicon, Temecula, CA); hamster anti-rat β1, clone HA2/5 (PharMingen); hamster anti-rat α5, clone HM 5–1 (PharMingen); mouse anti-human α5, clone IIA1 (PharMingen); polyclonal rabbit anti-αv (Chemicon); mouse anti-rat $\alpha6\beta1$ (Chemicon); polyclonal goat anti-rat FN (Calbiochem, San Diego, CA); polyclonal rabbit anti-human IgG_1 Fc (Sigma, Poole, UK); polyclonal anti-galanin (Peninsula Laboratories, Belmont, CA); and polyclonal anti-calcitonin gene-related peptide (CGRP; Peninsula).

α4 integrin immunohistochemistry in sensory ganglia and sciatic nerve. All operations were performed under anesthesia with tri-Brom-Ethanol (Avertin; Sigma), 0.4 mg/gm body weight, on 2- to 3-month-old mice. The animal experiments and care protocols were approved by the Regierung von Oberbayern (AZ 211-2531-10/93 and AZ 211-2531-37/97). The left sciatic nerve was cut or crushed at the sciatic notch, and the animals were killed in ether after 4 d. For dorsal root ganglia, the animals were flushed for 5 min with PBS (20 ml/min) then perfusion-fixed with 200 ml of 4% formaldehyde (FA) in PBS (4% FA–PBS). The L5 ganglia were removed from the operated and contralateral side, post-fixed in 1% FA–PBS for 2 hr, cryoprotected with 30% sucrose overnight, covered with OCT (Miles, Elkhart, IN), frozen on dry ice, and cut in a cryostat at −18°C. Twenty 20 μm longitudinal sections were collected on warm glass slides coated with 0.5% gelatin (Merck, Darmstadt, Germany), refrozen on dry ice, and stored at −80°C for further use. For immunohistochemistry on crushed sciatic nerves, the brief perfusion with PBS and 4% FA–PBS was followed by a slow, 60 min perfusion-fixation with 1% FA–PBS. The sciatic nerve was then immediately dissected for a length of 20 mm, covered with OCT, frozen on dry ice, and cut longitudinally at 10 μm thickness. Nerve and ganglia sections were processed for immunohistochemistry as described by Möller et al. (1996) and Werner et al. (2000). Briefly, the sections were dried, fixed in 4% paraformaldehyde in phosphate buffer (PB; 100 mM Na_2HPO_4, pH 7.4) for 5 min, washed twice in PB, and washed once in PB with 0.1% bovine serum albumin (PB–BSA; Sigma). DRG sections were preincubated for 1 hr with 5% goat serum in PB, incubated with a 1:1000 diluted rat monoclonal antibody R1–2 (PharMingen) against the α4 integrin subunit overnight at 4°C in PB–BSA, then with a biotinylated goat anti-rat secondary antibody (1:100 in PB–BSA; Vector Laboratories, Wiesbaden, Germany) for 1 hr at room temperature (RT), washed again (PB/BSA, PB/BSA, PB, PB), followed for 1 hr with ABC-reagent (Vector) in PB at RT, washed (PB, PB, PB, PBS), and finally visualized using diaminobenzidine (DAB; 0.5 gm/l in PBS; Sigma) with 0.01% H_2O_2 for 5 min at RT. The sections were then washed again, dehydrated in alcohol and xylene, and mounted in Depex. Digital micrographs of the brainstem were taken in a Zeiss Axiophot microscope with a 5× objective and a Sony 89B CCD (model CX-77CC) and imported into the Optimas 6.2 (Bothell, WA) imaging system using an Image Technology OFG card (VP-1100–768).

For axonal colocalization of the α4 integrin in the regenerating sciatic nerve, the fixed sections were preincubated with 5% donkey serum (Sigma) in PB and then simultaneously incubated overnight with the monoclonal α4 antibody (1:1000) and polyclonal rabbit antibodies against CGRP or galanin (1:600) from Peninsula. The sections were washed, incubated simultaneously with two secondary antibodies, biotin-conjugated donkey anti-rabbit Ig and FITC-conjugated goat anti-rat Ig or goat anti-hamster Ig and (1:100 in PB–BSA; Dianova, Hamburg, Germany), then washed again and incubated with a tertiary FITC-conjugated donkey anti-goat antibody (1:100 in PB–BSA; Sigma) and Cy3–Avidin (1:1000 in PB–BSA; Dianova) for 2 hr at RT. After washing, the sections were covered with VectaShield (Vector) and stored in the dark at 4°C for further use. For visualizing the immunofluorescence double-labeling, digital micrographs of the FITC for the integrin staining and the Cy3 fluorescence for the respective axonal marker representing an area of 50 by 50 μm (1024 × 1024 pixels; grayscale 0–255) were taken with a Leica TCS 4D confocal laser microscope using a 100× objective and 2× zoom. The fluorescence was excited using low Ar–Kr laser power (0.25 V) at wavelengths of 488 nm for FITC and 568 nm for Cy3 and detected using the BP–FITC filter for FITC and the LP590 filter for Cy3, respectively. Nine consecutive, equidistant levels spanning 10 μm were recorded and condensed to a single bitmap using the MaxIntens algorithm.

α4 integrin in situ *hybridization.* Adult (10- to 13-week-old) Sprague Dawley rats were anesthetized (50 mg/kg pentobarbital, i.p.), and the left sciatic nerve was exposed at the sciatic notch. The nerve was transected with iridectomy scissors, and it was ascertained that the transection was complete. All animal protocols were approved by the Institutional Animal Care and Use Committee of The University of Pennsylvania. Four

days after nerve injury, the animals were overdosed (with an intraperitoneal dose of pentobarbital), and perfused with saline followed by 4% paraformaldehyde in PBS. The L4 and L5 segment of the spinal cord, as well as the left and right L4 and L5 dorsal root ganglia were removed and placed in the same fixative overnight at 4°C. The tissues were rinsed in PBS, infiltrated in 20% sucrose in PBS, then embedded in OCT. Five-micrometer-thick sections were mounted on Superfrost Plus slides (Fisher Scientific, Pittsburgh, PA), and they were air-dried and stored at −80°C.

The cDNA for α4 was obtained by reverse transcription of total RNA extracted from rat spleen, using random hexanucleotides (first strand cDNA synthesis kit; Amersham Pharmacia Biotech, Arlington Heights, IL). Briefly, a 1157 bp fragment corresponding to the cytoplasmic domain and part of the extracellular domain of α4 was amplified by PCR using primers introducing *Bam*HI and *Sal*I sites: 3′ end primer; 5′-GCG CGC GTC GAC GCG TCA TCA TTG CTT TTG CTG-3′, 5′end primer; 5′-GCG CGC GGA TCC TAT CTT GCT GTT GGG AG-3′. The fragment was cloned into pBluescript KS and transcribed using the T3 and T7 promoters to generate antisense and sense cRNAs, respectively. The transcription reaction consisted of ~1 μg of linearized plasmid DNA template, 10 mM DTT, digoxygenin (DIG)–NTP labeling mix (Roche Products, Hertforshire, UK), 40 U of RNase inhibitor (Roche), and 20 U of T3 or T7 RNA polymerases in transcription buffer (Roche). The product was purified using nick columns, then precipitated, washed, and stored at −80°C in DEPC H_2O. Integrity of the RNA probes was verified by gel electrophoresis. For prehybridization, frozen sections were thawed at room temperature for 30 min, fixed with paraformaldehyde in PBS for 10 min, acetylated in a solution of 4× SSC, pH 8.0, containing 0.25% acetic anhydride and 0.1 M triethanolamine for 10 min at room temperature, dehydrated in ethanol, delipidated in chloroform, and air-dried. The labeled cRNA probe was dissolved to a final concentration of 125 ng/μl in the hybridization solution (50% v/v formamide, 4× SSC, 1× Denhardt's solution, 100 μg/ml herring sperm DNA, 100 μg/ml polyA, and 10% w/v dextran sulfate), and applied onto each slide under coverslips. Hybridization was allowed to proceed for 14–18 hr at +65°C. Slides were dipped into 4× SSC, and then coverslips were carefully removed. Slides were further washed 10 min in 1× SSC, then incubated 30 min with RNase A (Boehringer Mannheim, Indianapolis, IN) and 30 min in RNase A buffer alone at 37°C, washed three times for 40 min each at +65°C in 1× SSC, 50% formamide, 0.1% Tween 20 and two times for 30 min each in 100 mM maleic acid, 150 mM NaCl, 0.1% Tween 20, pH 7.5. RNA hybrids were visualized *in situ* by immunohistochemistry with alkaline phosphatase-conjugated anti-DIG antibody (Boehringer kit) according to the manufacturer's instructions, except that polyvinyl alcohol (10% w/v) was included in the final color reaction to increase sensitivity. Slides were then dehydrated in ethanol and xylene and mounted under coverslips in Eukitt medium (Agar Scientific Ltd., Stansted, UK).

Cloning specific domains of rat FN. The Signal-pIgplus vector for the mammalian production of fusion proteins with a C-terminal Fc tail (human IgG_1 Fc) was used. In addition to the Fc sequence, the vector includes the CD33 signal sequence to facilitate the secretion of the fusion proteins. FN fragments that begin and end precisely at the boundaries of individual type III domains were cloned into the vector. The various recombinant fragments contain the three possible combinations of the V region and encompass the type III repeats 8–15 and 11–15 (Fig. 1). The FN cDNA was obtained by reverse transcription of total RNA extracted from rat liver, using random hexanucleotides. Briefly, the fragments were amplified by PCR using primers with the appropriate restriction sites and cloned in frame into the *Nhe*I and *Not*I sites of Signal-pIgplus. All cDNA fragments obtained were sequenced.

Site-directed mutagenesis. The 8V120 FN fragment was subjected to site-directed mutagenesis using the Quikchange mutagenesis kit (Stratagene, La Jolla, CA) following manufacturer's instructions. The LDV sequence within V25 was mutated to LAV using the following primers: GGACCAGAGATCTTGG*C*TGTTCCCTCCACAG (sense) and the matching antisense strand. Base substitution at the site of mutation was confirmed by DNA sequencing. The fragment containing the mutated LAV sequence was excised with *Bam*HI–*Not*I and subcloned into 11V120 to create 11LAV.

Purification of recombinant FN fragments. The Signal-pIgplus expression vector allows for a purification strategy by affinity isolation on Protein A sepharose. COS7 cells were transiently transfected with recombinant DNA using the FuGENE 6 transfection reagent (Roche) according to manufacturer's instructions. After 24 hr of incubation the cells were washed twice with PBS, and the medium was replaced by chemically defined/Sato's serum-free medium for 2–3 d. The conditioned media were collected and loaded on a Protein A–Sepharose (Sigma) column. Recombinant FNs were eluted using 0.1 M citrate buffer at pH 3.5. The final concentrations were determined by UV absorption. Protein sizes were confirmed on SDS-PAGE as described by Laemmli. In addition, purified fragments were separated on 7% (8–15) and 10% (11–15) polyacrylamide gels and transferred to nitrocellulose membranes. The membranes were incubated with antibodies against rat FN and human IgG_1 Fc and revealed using ECL reagents (Amersham Pharmacia Biotech).

Protein adsorption assay. Briefly, 96-well tissue culture dishes were adsorbed for 3 hr with anti-IgG_1 Fc antibody, washed with PBS, and incubated overnight at 4°C with various concentrations of recombinant fragments in PBS. Wells were rinsed with PBS and postadsorbed for 1 hr with 3% heat-inactivated bovine serum albumin (BSA) in PBS and washed three times with PBS. Adsorbed polypeptides were quantitated using anti-pFN antiserum and an HRP-conjugated secondary antibody and OPD peroxidase substrate tablets (Sigma). Results were read on a PerkinElmer reader at 450 nm.

Cell culture. COS7 and NIH 3T3 cells were grown in DMEM supplemented with 10% fetal calf serum (FCS), penicillin–streptomycin, and 2 mM glutamine (Sigma).

Rat pheochromocytoma (PC12) cells were grown on poly-D-lysine-coated tissue culture flasks in DMEM supplemented with 10% horse serum (HS), 5% FCS, penicillin–streptomycin, and 2 mM glutamine. For priming with NGF, PC12 cells were passaged onto collagen-coated (calf skin collagen; Sigma) Petri dishes at a density of 10^4 cells/cm^2 and cultured for 4–5 d in DMEM complemented with 1% ITS^+ premix (Collaborative Research, Bedford, MA) and 50 ng/ml 2.5S NGF (Serotec, Oxford, UK). For neurite outgrowth assays, NGF-primed cells were passaged by gentle trituration and cultured on the desired substrate in the same defined medium.

Individual DRGs from newborn Sprague Dawley rats (P1 or P2) were dissected into Ca^{2+}, Mg^{2+}-free HBSS and incubated with 0.25% trypsin for 30 min at 37°C. Ganglia were dissociated by trituration, and cells were washed twice in DMEM supplemented with 10% FCS to stop the reaction. The cell suspension was then enriched for neuronal cells by preplating for 60 min in 35 mm dishes. The unattached neurons were then collected, washed, gently centrifuged, and either used directly for neurite outgrowth assays or for long-term DRG neuron cultures. For DRG cultures, the neurons were plated onto FN-coated (plasma FN; Sigma) 90 mm tissue culture dishes. The culture medium consisted of DMEM supplemented with Ultroser G serum substitute (Life Technologies, Gaithersburg, MD), 0.1× B27 (Life Technologies), 2 mM glutamine, penicillin–streptomycin, 50 ng/ml 2.5 S NGF, and 40 μM AraC. For neurite outgrowth assays, the medium solely consisted of DMEM complemented with 2 mM glutamine, penicillin–streptomycin, 1% ITS^+ premix, and 50 ng/ml 2.5 S NGF.

Neurite outgrowth assay. All neurite outgrowth assays were performed in 4-well tissue culture plates. For preparation of the substrates, ligands were diluted into PBS and deposited as 30 μl drops in the center of the wells. The dishes were first coated with 10 μg/ml anti-IgG_1 Fc for 4 hr at RT, washed two times with PBS, and then postadsorbed with the various fragments overnight at 4°C. The wells were washed three times with PBS, and neurons or PC12 cells were deposited in 30 μl drops on the substrates at a density of 5×10^2/cm^2. After 1 hr, when the cells were attached and the medium was added to a final volume of 200 μl. In perturbation experiments, GRGDSP peptides (Life Technologies) were added to the medium to a final concentration of 0.1 μg/ml. To monitor the efficacy or toxicity of the peptides, parallel control experiments without any additive and with inactive GRGESP peptides were conducted.

Analysis of neurite outgrowth. Measures were taken after 24 and 48 hr (separate sets of dishes). Dishes were viewed under a Zeiss phase microscope, and random fields were recorded on videotape. The percentage of neurons with at least one neurite equal or greater than one cell body diameter in length was determined relative to the total population of attached neurons. The approximate length of the single longest neurite was also determined. Determinations were made on at least five separate experiments; for percentages of neurons bearing neurites, >100 neurons per culture were counted, and for neurite lengths measurements at least 50 neurons per well were measured. For the experiments using PC12 cell lines, untransfected and mock-transfected cells were used as negative controls. Assays were conducted on both experimental and control cell lines in parallel, and the results were normalized to the

control values. Each assay was repeated five times, and the mean was determined. In addition, for experiments on transfected PC12 cells, the assays were also repeated with three independently generated cell lines. Statistical analysis was performed using Student's *t* test.

Construction of integrin chimeras. cDNAs encoding the wild-type human α4 and human α5 chains were gifts from M. E. Hemler (Dana-Farber Cancer Institute, Boston, MA) and R. Horwitz (University of Virginia, Charlottesville, VA), respectively. Generation of truncated α integrin subunits and chimeric α integrins containing the extracellular and transmembrane domain of the α5 chain and the cytoplasmic domains of either α4 or α6 is described in detail elsewhere (Relvas et al., 2001). Briefly, a cytoplasmic truncation of the α5 chain was performed by the ligation to the *Hin*dIII site immediately preceding the GFFKR motif of a synthetic double stranded oligonucleotide encoding the GFFKR sequence followed by a stop codon. The truncation of the α4 chain was performed by site-directed mutagenesis to introduce a stop codon after the GFFKR, using the primer GG AAG GCT GGC TTC TTT AAA AGA *T*AA TAC AAA TCT ATC CTA CAA G (sense). To generate the α5α4 and α5α6 chimeras, the cytoplasmic tail of the human α5 sequence was excised using the *Hin*dIII site immediately preceding the GFFKR motif. The α4 and α6 cytoplasmic tails, starting from the GFFKR motif, were amplified by PCR, introducing a *Hin*dIII restriction site at the 5′ end and a *Sal*I site at the 3′ end. Amplified tails were cloned in frame of the α5 extracellular sequence into the *Hin*dIII restriction site. All cDNAs obtained were sequenced. The integrin sequences were then excised with *Sal*I and subcloned into the *Xho*I site of the bicistronic retroviral vector pLXIN (Clontech, Palo Alto, CA).

Transfection and selection of stable clones. The constructs were transfected into the GP+86 packaging cell line, using FuGENE 6 as transfection reagent. Cells were maintained in DMEM supplemented with 10% FCS, penicillin–streptomycin, 2 mM glutamine, and 1 mg/ml G418 (Life Technologies) until clones appeared. The GP+86 cells were then replated and when at 60–70% confluence, were washed, and medium without G418 was added. The conditioned medium was collected after 24 hr, filtered (0.45 μm pore size), and either used immediately or aliquoted, frozen, and kept at −70°C. Virus titer was determined using NIH 3T3 cells. PC12 cells were infected in the presence of polybrene and selected and maintained with 1 mg/ml G418.

Cell labeling and immunoprecipitation. Cell surface molecules were labeled with 0.1 mg/ml NHS–LC–biotin (Pierce) in PBS at 37°C for 30 min. Cells were washed three times with cell wash buffer (50 mM Tris-HCl, pH 7.5, 0.15 M NaCl, 1 mM $CaCl_2$, and 1 mM $MgCl_2$), scraped, and lysed on ice for 30 min in extraction buffer (cell wash buffer plus 1% Triton X-100, 0.05% Tween 20, 2 mM PMSF, 1 μg/ml pepstatin A, 2 μg/ml aprotinin, 5 μg/ml leupeptin, 2 mM sodium vanadate, 2 mM sodium fluoride, and 4 mM sodium pyrophosphate). After centrifuging at 14,000 rpm for 20 min at 4°C, the insoluble pellet was resuspended using a syringe with a 25 gauge needle in 100 μl of solubilization buffer composed of 10 mM Tris-HCl, pH 7.4, 10 mM NaCl, 3 mM $MgCl_2$, 1% Triton X-100, 0.5% SDS, 1 mM PMSF, 1 μg/ml pepstatin A, 2 μg/ml aprotinin, and 5 μg/ml leupeptin. The cell lysates were incubated with 30 μl protein A-Sepharose (Amersham Pharmacia Biotech). The lysates were precleared by two sequential 2 hr incubations, and immunoprecipitations were performed overnight at 4°C. When hamster or mouse monoclonal antibodies were used, rabbit anti-hamster or rabbit anti-mouse antisera (Nordic Immunological Laboratories) were also added to the tubes. All antibodies were used at a dilution of 1:250. The beads were washed five times with immunoprecipitation buffer (identical to cell wash buffer except for 0.5 M NaCl and 1% NP-40), and the precipitated polypeptides were extracted with SDS sample buffer. Precipitated cell surface biotin-labeled molecules were separated by SDS-PAGE under nonreducing conditions and detected with streptavidin–peroxidase followed by ECL (Amersham Pharmacia Biotech).

Cell adhesion assay. Ninety-six-well plates were coated overnight at 4°C with 200 μl of PBS containing protein ligands. The wells were washed with PBS and blocked for 1 hr with 3% heat-denatured BSA. The wells were washed again, and 1×10^5 or 5×10^4 primed PC12 cells (in a 100 μl of cell suspension) were added per well and incubated for 30 min at 37°C. The wells were then washed two times with DMEM, fixed for 15 min with methanol, and stained with a 0.2% solution of crystal violet in 2% ethanol. The wells were washed once with H_2O, the crystal violet stain was solubilized in 50 μl of a 1% solution of SDS, and adhesion was quantitated by measuring the absorbance at 570 nm. Results are reported as the mean with the SD. Background cell binding to BSA was subtracted. Results are expressed relative to the reference value of 100% adhesion. To estimate this reference value, a 100 μl of cell suspension was centrifuged. The pellet was fixed, stained, washed, resuspended in 50 μl of 1% SDS, and absorbance was measured. All experiments were repeated at least three times.

RESULTS

α4 integrin in sensory ganglia neurons and regenerating sciatic nerve

Previous immunohistochemical studies on integrins in the normal and injured mouse CNS revealed strong α4 immunoreactivity on the activated microglial cells (Kloss et al., 1999) but no specific labeling on the neighboring brainstem neurons after systemic treatment with lipopolysaccharide (Kloss et al., 2001) or on facial motorneurons after peripheral axotomy (Kloss et al., 1999). As shown in Figure 2*A*, however, there is strong α4 immunoreactivity on the cell bodies of peripheral sensory neurons in the dorsal root ganglia. Both small- and large-caliber sensory neurons were α4-positive, and this cellular pattern and the staining intensity did not change after transection of the sciatic nerve (Fig. 2*B*). Motorneurons in the spinal cord did not show α4 immunoreactivity (data not shown).

In addition to these studies on protein expression, we also examined the effect of transection on α4 mRNA expression. We performed *in situ* hybridization experiments with antisense and sense rat α4 probes using rat tissue, as described in Materials and Methods. Consistent with our experiments showing no change in protein expression after axotomy, we also found no change in the pattern of α4 mRNA expression, with both large- and small-diameter neurons labeled in the DRG (Fig. 2*C–E*). The small-diameter neurons showed greater levels of α4 mRNA than the larger diameter neurons, as judged by staining intensity (Fig. 2*C,D*), but this semiquantitative technique revealed no changes in overall expression levels after injury. As expected from the immunohistochemical studies, we also found no expression of α4 mRNA in spinal cord motorneurons (data not shown).

To confirm the presence of the α4 immunoreactivity on the regenerating axons, the mouse sciatic nerve was crushed, and the distal part of the nerve, 4–6 mm below the crush site, was examined by immunohistochemistry and confocal microscopy 4 d after injury. At high magnification, α4 immunoreactivity was present in discrete foci of ~0.5 μm diameter that were aligned longitudinally like pearls on a bead (Fig. 2*F,H*). Double staining with antibodies against the neuropeptides CGRP or galanin, present in large subpopulations of axotomized sensory neurons (Dumoulin et al., 1991; Zhang et al., 1998), frequently revealed an association of α4 with CGRP or galanin-labeled axons or growth cones (with the latter shown in Fig. 2*F–I*). These observations therefore demonstrate the expression of α4 on the regenerating growth cones in the injured nerve.

Neurite outgrowth of DRG neurons on recombinant FN fragments

Having demonstrated expression of α4 on DRG neurons *in vivo*, we next analyzed the role of this integrin in neurite extension. To do this, we made recombinant FN fragments with or without either the V25 region or the RGD sequence and used them as substrata for DRG neurons.

A total of eight different rat FN fragments were used in this study, and their nomenclature is shown in Figure 1. Fragments were made to either include both the central cell binding domain located within 10th type III repeat together with the three possible combinations of the alternatively spliced V region or to include only the V region isoforms. We therefore chose to span

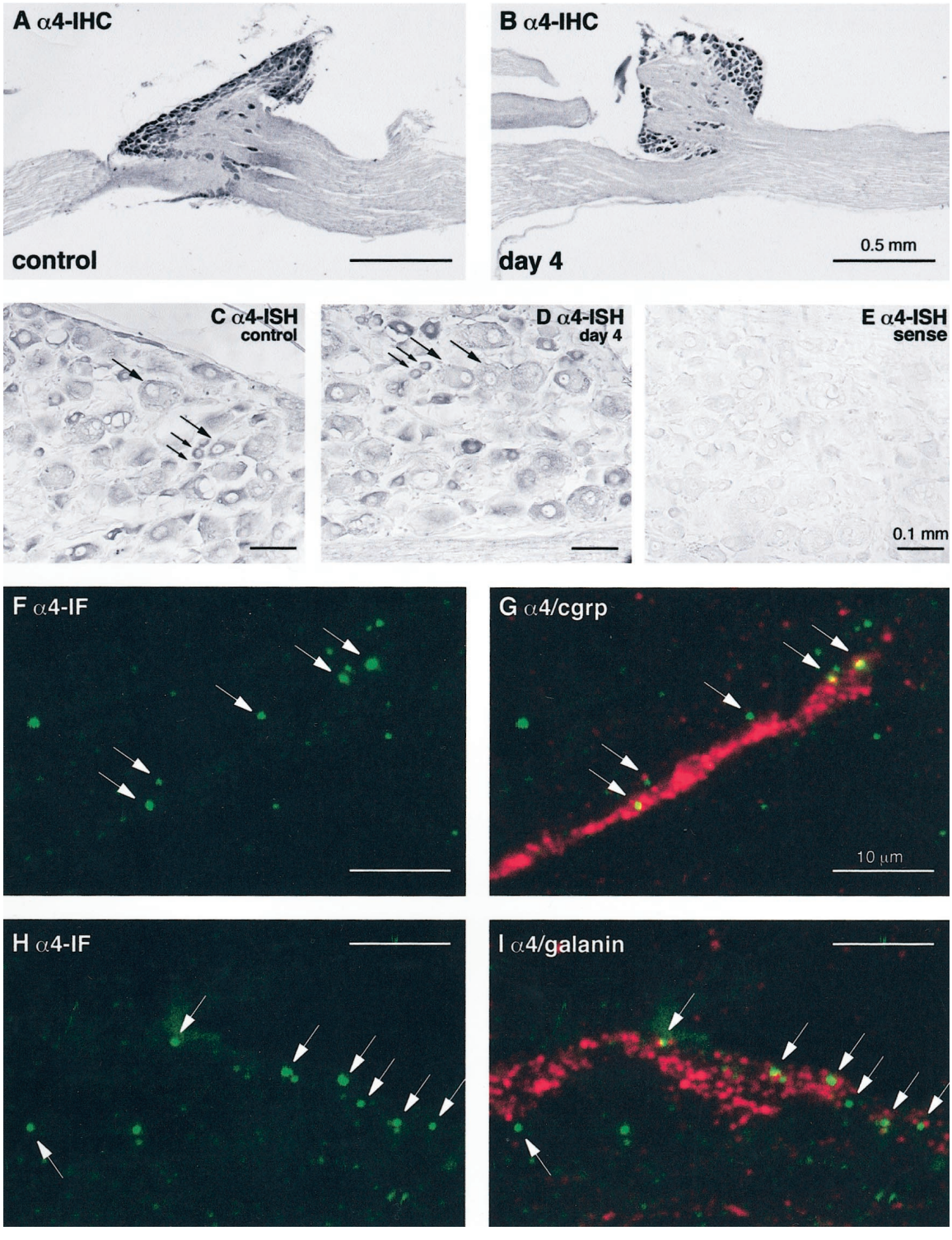

Figure 2. α4 integrin expression after sciatic nerve injury in mouse and rat. *A* and *B* show α4 immunoreactivity visualized by immunoperoxidase in the L5 spinal ganglia 4 d after axotomy of the mouse sciatic nerve. Note that α4 is expressed within the DRG neurons on both the control, unlesioned (*A*), and lesioned (*B*) side, without any changes in expression level. *C–E* show the effects of axotomy on α4 mRNA levels in rat sciatic nerve, as assessed by *in situ* hybridization on sections of DRG neurons from the experimental (*C, E*) and control (*D*) side. *C* and *D* show the expression of α4 mRNA in both large- and small-diameter neurons (*large* and *small arrows,* respectively) both before (*C*) and 4 d after axotomy (*D*). *E* shows a sense control with no nonspecific hybridization. *F–I* represent higher power confocal images showing α4 immunoreactivity (*green*) and either CGRP or Galanin (*red*) in the distal stump 4 d after sciatic nerve crush. These show the presence of discrete foci of α4 associated with growth cones marked by CGRP or galanin immunoreactivity, confirming the presence of this integrin in regenerating nerves. Note that some of the α4 immunoreactivity in these confocal images is seen at the edge of the CGRP–galanin-labeled areas, as would be expected given the cell surface expression of α4 integrin and the cytoplasmic localization of CGRP or galanin within the growth cones.

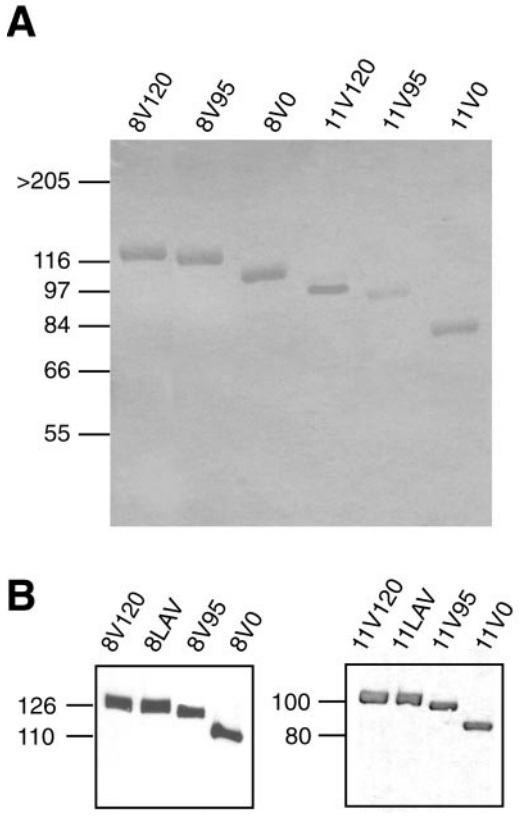

Figure 3. SDS-PAGE and immunoblot analyses of recombinant fragments. *A,* Recombinant FN fragments purified on protein A-Sepharose columns, as described in Materials and Methods, were subjected to SDS-PAGE under reducing condition and visualized by Coomassie staining. Molecular weight markers are shown on the *left*. Note that all fragments appear as single bands. *B,* Purified FN fragments (0.5 μg/lane) were subjected to SDS-PAGE under reducing conditions followed by immunoblotting with polyclonal anti-Fc antibody. *Left*, 8–15 fragments. *Right*, 11–15 fragments.

repeats 8–15 (to include the RGD sequence in repeat number 10) or 11–15 (to exclude the RGD sequence), all without inclusion of the alternatively spliced EIIIA exon. The FN fragments were generated by RT-PCR from rat liver and cloned as described in Materials and Methods. FN fragments were expressed as chimeric proteins with the signal sequence of CD33 and a C-terminal Fc tail (human IgG_1 Fc), as described in Materials and Methods. The Fc tail will allow dimerization of the fragments, thereby better mimicking the dimer conformation of soluble, plasma-derived FN *in vivo*. The purified proteins gave single bands after SDS-PAGE and Western blot analysis under reducing conditions (Fig. 3). The relative molecular masses of FN fragments were consistent with the expected sizes. All recombinant proteins were reactive toward anti-Fc and anti-FN antibodies (Fig. 3).

Whole dorsal root ganglia or dissociated DRG neurons from newborn rats [postnatal day 1 (P1)–P2] were then seeded onto 4-well plates coated with an antiserum to IgG_1 Fc, followed by equimolar concentrations of recombinant FN fragments. In previous control experiments the binding of recombinant fragments to the dishes precoated with anti-Fc antibodies was evaluated quantitatively by ELISA, using a polyclonal goat antiserum to FN. Saturation of surfaces did not vary significantly from protein to protein, and all proteins saturated at concentrations >5 μg/ml (data not shown). For routine experiments, substrata were adsorbed with 10 μg/ml of antiserum to IgG_1 Fc, followed by 50 nM of recombinant proteins (~5 μg/ml for 8–15 fragments). DRG neurons extended neurites on FN in a time-dependent manner, and the rate of outgrowth was linear for 48 hr (Fig. 4*A*). Throughout these studies, whole ganglia and dissociated neurons yielded essentially the same results, and therefore only the results for dissociated neurons are shown. The rate of outgrowth of the dissociated cells was, however, strongly dependent on cell density. To facilitate quantitation, and also to avoid fasciculation, neurons were seeded at the low surface density of $5 \times 10^2/cm^2$.

Neurite outgrowth was greatest on the V120-containing fragments. Neurite length on 8V120 was twice that on 8V95 and 8V0 (Fig. 4*A,B*). When RGD peptides were added to the medium as competitive inhibitors of the RGD binding site in the 10^{th} repeat, neurite outgrowth was nearly abolished on 8V95 and 8V0, but not on 8V120, which retained a reduced outgrowth-promoting activity (Fig. 4*B*). Control Arg-Gly-Glu (RGE) peptides had no effect. On fragments lacking the main cell-binding site, neurons extended neurites on 11V120 but not on 11V95 and 11V0, and RGD peptides had no effect on neurite outgrowth (data not shown). Interestingly, 11V95 supported weak outgrowth, whereas outgrowth on 11V0 was no greater than BSA-blocked, IgG_1 Fc-coated plastic. The percentages of cells extending neurites on the different substrates mirrored precisely their neurite lengths. Forty-one percent of neurons extended neurites on 8V120, as opposed to 28 and 25% on 8V95 and 8V0, respectively.

These experiments show that, in keeping with previous results using V25 peptides and proteolytic fragments of FN (Humphries et al., 1988), both the RGD sequence and the V25 region promote neurite outgrowth in an additive manner. To confirm that the neurite outgrowth-promoting activity of V25 containing fragments resides in the α4β1 binding sequence LDV, we mutated this sequence to LAV (8LAV), as described in Materials and Methods. The increased outgrowth observed on 8V120 was abolished on 8LAV. 8LAV supported the same neurite outgrowth-promoting activity as 8V95 and was blocked to the same extent by RGD peptides (Fig. 4*C*). Similarly, 11LAV supported only weak neurite outgrowth, as previously found with 11V95.

Comparison of neurite outgrowth and integrin expression in PC12 cells and DRG neurons

To examine integrin function further in PNS neurons we switched to the use of the PC12 cell line to facilitate the use of genetic manipulation to express different integrin subunits. PC12 cells are known to adhere well to laminin and type IV collagen but to attach poorly to FN (Tomaselli et al., 1987). As expected, therefore, we found that PC12 cells extended relatively short neurites on FN when compared with DRG neurons (Fig. 5*A*). This appeared to be mediated by RGD-binding integrins, because neurite outgrowth was nearly completely blocked on all 8–15 fragments by RGD peptides (Fig. 5*B*). In contrast to the DRG neurons, the V25 fragment showed no enhanced neurite-outgrowth promoting activity in PC12 cells, because 8V120 showed no greater neurite outgrowth-promoting activity than 8V95 and 8V0. Moreover, 11V120, like 11V95 and 11V0, was totally ineffective at promoting neurite outgrowth (data not shown).

These results showing that the PC12 cells do not respond to the V25 segment suggested that DRG neurons would express both α4β1 and α5β1, whereas PC12 cells would express only α5β1. We found that the antibodies used against α4 and α5 integrins worked poorly in Western blotting studies, and the endogenously ex-

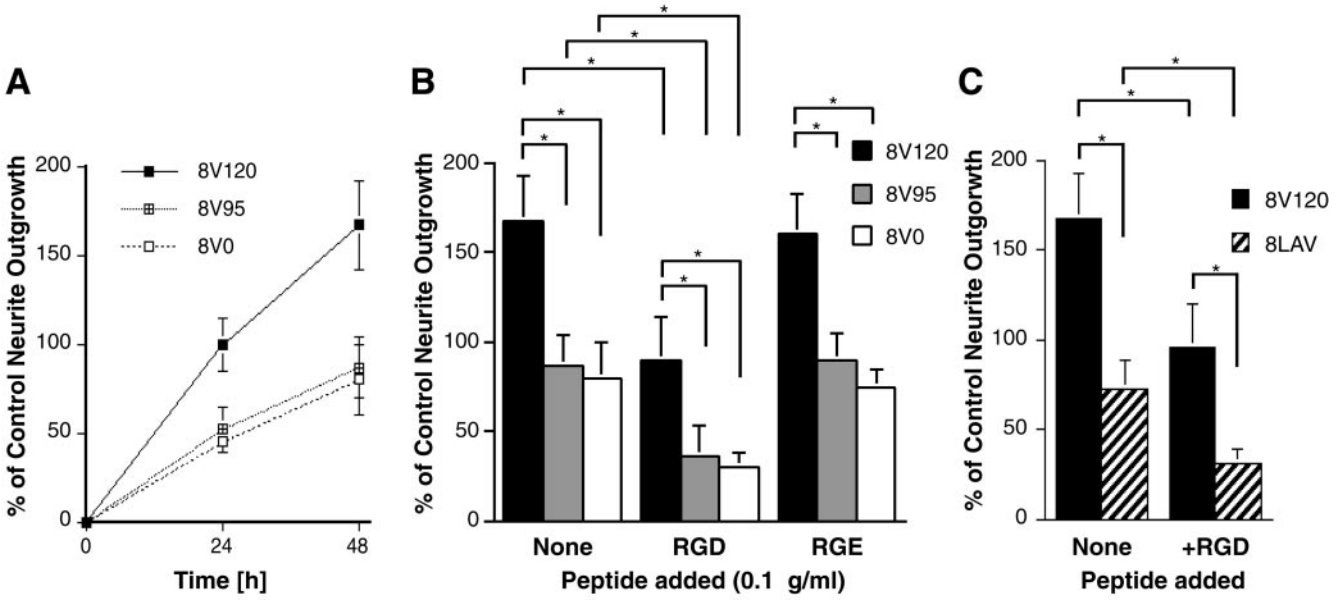

Figure 4. Effect of the V region on neurite outgrowth of DRG neurons. Neurons were plated on the three different 8–15 fragments, as described in Materials and Methods. Neurite outgrowth was quantitated after 24 and 48 hr. In each experiment at least 50 neurons were measured, the median was determined, and the values were normalized relative to the neurite outgrowth on 8V120 after 24 hr. Data represent the mean from five separate experiments ± SEM. *A,* Neurite outgrowth of DRG neurons over 48 hr. *B,* Neurite outgrowth of DRG neurons after 48 hr on 8V120, 8V95, and 8V0 ± 0.1 μg/ml RGD or RGE peptides. Note the enhanced neurite outgrowth on V120 isoforms (*$p < 0.01$). *C,* Neurite outgrowth of DRG neurons on 8V120 and 8LAV, after 48 hr, ± RGD peptides. Note the enhanced neurite outgrowth on V120 isoforms is abolished when the LDV sequence within V120 is mutated to LAV (*$p < 0.01$).

pressed integrins in DRG or PC12 cultures were therefore analyzed by immunoprecipitation of detergent extracts of surface-biotinylated cells as described in Materials and Methods. This method also ensures that only integrins expressed on the cell surface are identified. In non-reducing SDS-PAGE, immunoprecipitations of rat DRG neuronal cultures with anti-α5, anti-α4, and anti-β1 identified biotin-labeled subunits with the expected mobilities of α5β1 and α4β1 (Fig. 5*C*). In contrast and as predicted, PC12 cells did not express any detectable endogenous integrin α4 subunit, and the level of α5 expression was very low (Fig. 5*D*). In comparison, α1, α6, α3, and αv are all strongly expressed, consistent with previous studies, with α1β1, α3β1, and α6β, representing the predominant β1 integrins (Tomaselli et al., 1990).

Effects of integrin expression on PC12 neurite outgrowth

The lack of endogenous α4 integrin on the PC12 cells and the consequent lack of V25-stimulated outgrowth allows the use of exogenous α4 expression to determine the function of this integrin. We therefore generated stable cell lines expressing either full-length human α4 (α4α4) or a truncated α4 (cytoplasmic tail deletion: α4a0). Analysis of α4 expression by immunoprecipitation using an anti-α4 monoclonal antibody (mAb) yielded similar levels of α4 and β1 proteins for each transfectant (Fig. 6*A*). In addition, an anti-β1 mAb immunoprecipitated the transfected α4α4 or α4a0 in association with β1 (data not shown), confirming the formation and expression on the cell surface of α4β1 heterodimers in both lines. In neurite outgrowth assays, α4α4 restored in PC12 cells the significantly increased outgrowth seen in DRG neurons on both 11V120 and 8V120, and RGD peptides did not block this effect (Fig. 6*B*). As expected, this effect was not seen on V95 or V0 isoforms lacking V25 (Fig. 6*B*) or on the 8LAV and 11LAV isoforms (data not shown), confirming the specificity of the exogenously expressed α4β1 integrin for the LDV sequence in V25. In contrast to the full-length α4α4, the cytoplasmic domain truncated α4a0 had no effect on outgrowth as compared to mock-transfected and untransfected PC12 cells (Fig. 6*B*).

These results show that the expression of α4 is sufficient to restore to PC12 cells the ability to respond by enhanced neurite outgrowth to V25-containing forms of FN and suggests that this response requires the α4 cytoplasmic domain. To confirm the necessary role of the α4 cytoplasmic domain, we used a chimeric integrin strategy taking advantage of the specificity of the α5β1 integrin for the RGD sequence. If the α4 cytoplasmic domain is sufficient for neurite outgrowth promotion, then an α5α4 chimera should promote enhanced outgrowth on all FN substrata and not just on those containing the V25 region as with the α4α4 integrin. Full-length human α5 (α5α5), truncated α5 (cytoplasmic tail deletion; α5a0), a chimeric α5 containing the cytoplasmic domain of α4 (α5α4) and a chimeric α5 with the tail of α6 (α5α6) were therefore expressed on the surface of PC12 cell lines. Equivalent levels of expression were confirmed by immunoprecipitation, and all α5 subunits were shown to heterodimerize with β1 (Fig. 7*A*) (data not shown for α5α6). As expected, the three different substrates 8V120, 8V95, and 8V0 now all promoted neurite outgrowth equally for all transfectants (data not shown), because all contain the RGD sequence recognized by the α5β1 integrin extracellular domains expressed on all the cell lines. However, the four cell lines showed significant differences in their ability to support neurite outgrowth, because PC12 cells transfected with α5α4 extended significantly longer neurites than α5α5, α5α6, and α5a0 (Fig. 7*B,C*). These differences do not reflect changes in adhesion: in 30 min adhesion assays the α5α5, α5a0, α5α4, α5α6 molecules all supported similar adhesion on both 8–15 fragments and whole plasma FN (Fig. 7*D*). Adhesion was increased as compared with untransfected and mock-transfected PC12 cells on

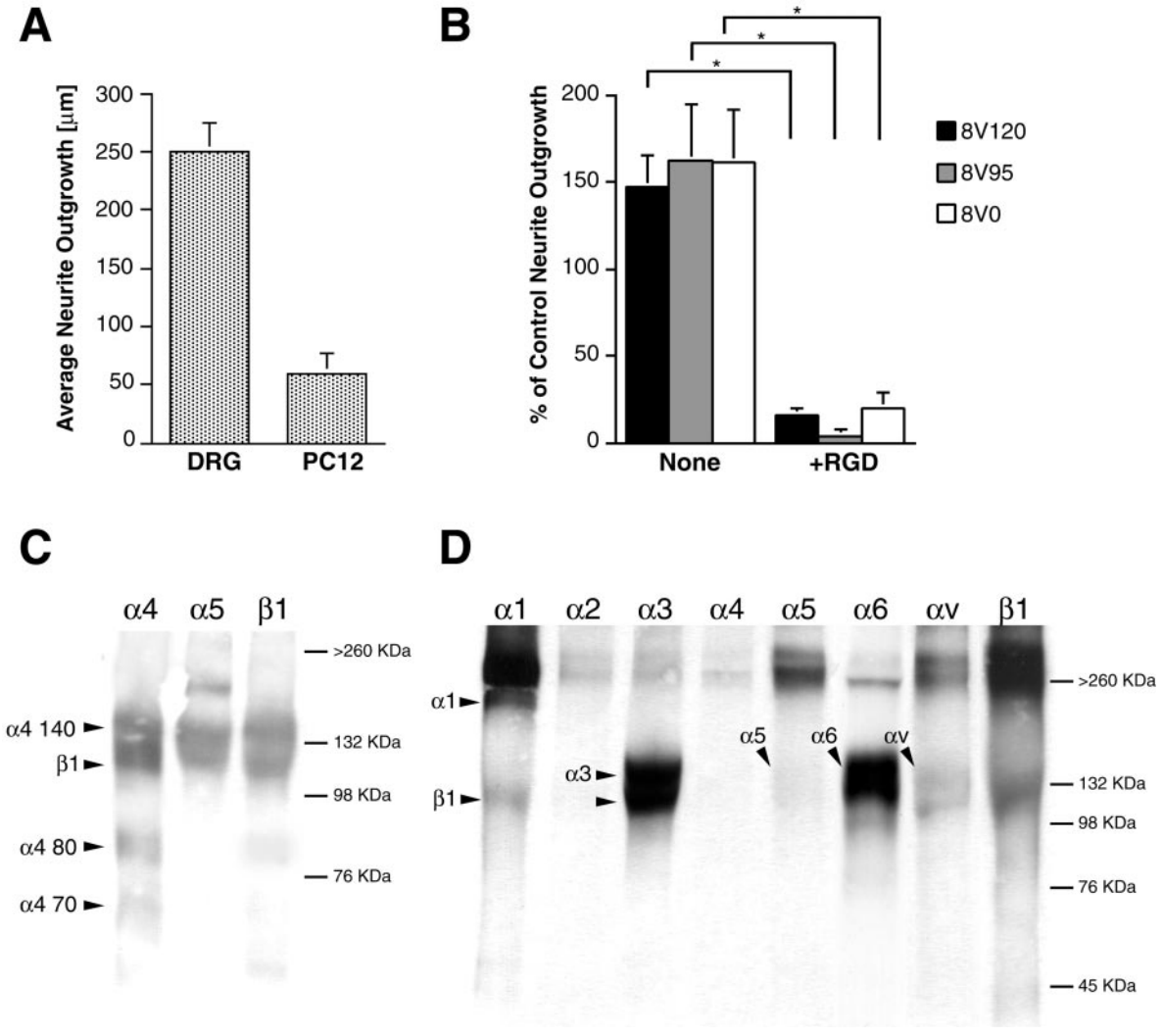

Figure 5. Integrin function and expression in DRG neurons and PC12 cells. *A,* Direct comparison of neurite outgrowth of DRG neurons and PC12 cells on FN after 24 hr. *B,* Effect of the V region on neurite outgrowth of PC12 cells. PC12 were plated on 8V120, 8V95, and 8V0, ± RGD peptides, and neurites were measured after 24 and 48 hr. In each experiment the neurites of at least 50 cells were measured, the median was determined, and the values were normalized relative to the neurite outgrowth on 8V120 after 24 hr. Data represent the mean outgrowth at 48 hr from five separate experiments ± SEM. Note that PC12 cells do not show increased neurite outgrowth on V120-containing fragments and that outgrowth on all fragments is essentially completely blocked with RGD peptides ($^*p < 0.01$). *C,* Cell lysates from DRG neurons (surface-labeled with biotin) were precipitated with anti-α4 Ab, anti-α5 Ab, and anti-β1 Ab. Immunoprecipitated proteins (equal amounts of protein were loaded) were separated by SDS-PAGE on 7% gels under nonreducing conditions, transferred to a nitrocellulose membrane, and detected with streptavidin peroxidase and ECL. Note that the neurons express both α4β1 and α5β1. *D,* Cell lysates from PC12 cell (surface-labeled with biotin) were immunoprecipitated with anti-α1, anti-α2, anti-α3, anti-α4, anti-α5, anti-α6, anti-αv, and anti-β1 antibodies and visualized as with the DRG neurons. Note that PC12 cells express low levels of α5 but no α4.

FN, as expected given the expression of α5β1, but no changes were seen in adhesion regulated by other integrins to collagen and laminin (data not shown).

Association of paxillin with the α4 cytoplasmic domain

These results confirm an instructive role for the α4 cytoplasmic domain in the signaling events that enhance neurite outgrowth in PC12 cells. In light of recent experiments showing that the adapter protein paxillin is associated with the α4 cytoplasmic domain in non-neural cells (Liu et al., 1999) and that expression of mutant forms of paxillin can inhibit neurite formation in PC12 cells (Ivankovic-Dikic et al., 2000), we next asked whether paxillin was associated with α4 in neurons. We therefore immunoprecipitated cell extracts from DRG neurons (generated using Triton X-100 detergent as described in Materials and Methods) with antibodies against α4, α5, or β1 integrin and then analyzed the precipitated proteins for the presence of coimmunoprecipitated paxillin by Western blotting with anti-paxillin antibodies. As shown in Figure 8*A*, two paxillin bands (presumably representing different isoforms) were seen in the α4 immunoprecipitation, whereas no bands were seen following immunoprecipitation with anti-α5 or anti-β1. This suggests that paxillin is specifically associated with α4 but not α5 in DRG neurons. To confirm this we performed two further sets of experiments. First, we immunodepleted DRG cell extracts with either anti-paxillin or anti-integrin antibodies and then asked to what extent the partner was also depleted after removal of the targeted protein from the lysate. As shown in Figure 8*B*, depletion with anti-α4 significantly reduced the level of paxillin within the remaining lysate, whereas anti-α5 had no effect. Similar results were obtained in the converse experiment, in which levels of α4 and α5 were analyzed in the

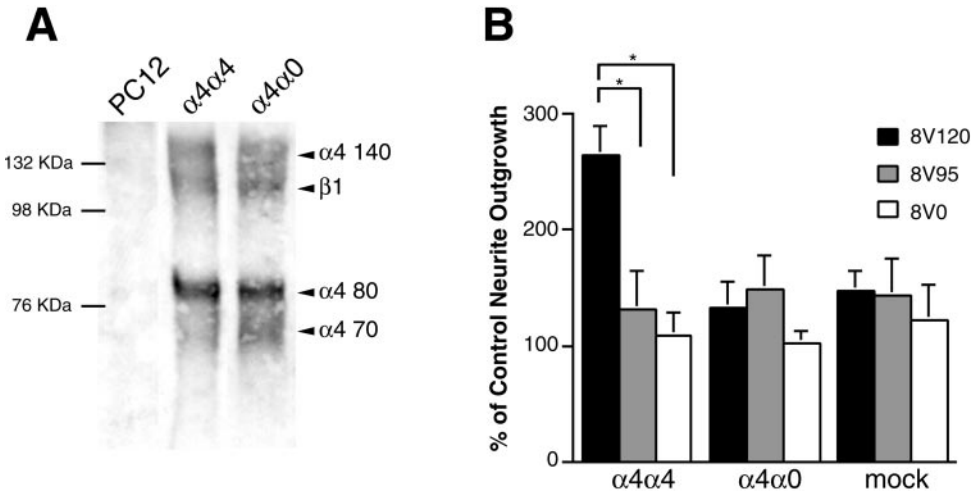

Figure 6. Effect of α4 transfection on the neurite outgrowth of PC12 cells. *A,* PC12 cell lines expressing α4α4 and α4α0 chains were surface-labeled with biotin and extracted with 1% Triton X-100. Immunoprecipitations were performed on equal amounts of protein with anti-human α4 antibody. Note that the full-length and truncated integrin are expressed at similar levels. Because the deletion only lacks 24 of the 999 amino acids in α4, no size difference would be expected at this resolution. α4 80 and 70 represent two products generated by post-translational cleavage of α4. *B,* Neurite outgrowth of PC12 cells stably transfected with α4α4, α4α0, or vector alone on 8V120, 8V95, and 8V0. Neurites were measured after 24 and 48 hr. In each experiment the neurites of at least 50 cells were measured, the median was determined, and the values normalized to control neurite outgrowth on 8V120 after 24 hr. Data represent the mean outgrowth at 48 hr of five separate experiments ± SEM. Note that the full-length, but not the truncated, α4 subunit restores increased neurite outgrowth of PC12 cells on V120-containing fragments ($^*p < 0.01$).

remaining lysate after paxillin immunodepletion (data not shown). Second, we re-immunoprecipitated proteins obtained after immunoprecipitation of cell extracts with anti-paxillin antibodies and found that α4 but not α5 was present in the proteins precipitated by the anti-paxillin antibodies (Fig. 8*C*).

To examine the association of paxillin with α4 in PC12 cells, we performed immunoprecipitation experiments using anti-α4 antibodies on extracts of the cell lines expressing full length α4α4 or truncated α4a0 and then Western blotted the precipitated proteins with anti-paxillin antibodies. Paxillin was present in the lysates from cells expressing full-length α4, but was not seen in the lysates from cells expressing the α4 cytoplasmic domain deletion (Fig. 8*D, lanes 1, 2*). To confirm the requirement for the cytoplasmic domain we repeated these experiments in the cell lines expressing the different α5 chimeras, now using an anti-α5 antibody for the immunoprecipitation step. Only in the cells expressing the α4 cytoplasmic domain did we observe paxillin within the precipitated proteins (Fig. 8*D*), confirming that the specificity of this interaction requires only the α4 cytoplasmic domain and is not dependent on the extracellular domain of the α subunit.

DISCUSSION

Our studies on the expression and function of integrins during peripheral nerve regeneration and neurite outgrowth are significant for three reasons. First, they show for the first time that the α4 integrin subunit is expressed on regenerating growth cones *in vivo*. Second, they show how alternative splicing of an extracellular matrix molecule after injury in the PNS can generate an environment that enhances repair. Third, they provide the first insights into the components of an intracellular signaling pathway activated by these changes in alternative splicing that are likely to play an important role in PNS regeneration.

Function of α4 integrin during nerve regeneration

A role for integrins in growth cone movement during neural development and repair has been suggested by cell culture studies examining neurite outgrowth on different ECM components (Reichardt and Tomaselli, 1991). Previous work has identified the α5β1 FN receptor and the α7β1 laminin receptor on growth cones *in vivo* (Lefcort et al., 1992; Werner et al., 2000). Transgenic mice lacking α7β1 show impaired axon regeneration in the facial nerve, confirming an important role for this integrin in regeneration (Werner et al., 2000). The embryonic lethality of the α4-deficient mice (Yang et al., 1995) prevents a transgenic analysis of α4 function in regeneration, and we have therefore used a combination of *in vivo* localization and *in vitro* neurite outgrowth assays to address the role of this integrin. Our present results now show for the first time that the α4 integrin is also expressed on a subset of regenerating axonal growth cones. Previous studies in the adult have suggested that α4 expression is confined to cells of the immune system, although developmental studies have revealed a much wider expression pattern in embryonic tissue including neural crest-derived cells and retinal neurons (Sheppard et al., 1994; Stepp et al., 1994; Kil et al., 1998). Our results showing expression of α4 on DRG neurons in both uninjured and axotomized nerve shows that expression is maintained on these neural crest-derived cells in the adult. The α4 integrin subunit can heterodimerize with either β1 or β7. The β1 subunit is expressed on regenerating growth cones, whereas β7 has only been reported in cells of the immune system and endothelial cells (Brezinschek et al., 1996; Wagner et al., 1996). We conclude, therefore, that the α4β1 heterodimer is expressed on regenerating growth cones in the peripheral nervous system and is likely to represent the major, if not only, α4 integrin present.

Although both α4 and α7 integrins are expressed in DRG neurons during regeneration, our data show two interesting differences between the regulation of these two integrins in response to injury. First, α7 is expressed on motorneurons and on some small-caliber sensory neurons, with mostly unmyelinated axons. Large-size sensory neurons, with myelinated axons, are α7-negative. In contrast, the α4 integrin appears to be confined to large and small sensory neurons, with no labeling seen in spinal cord motorneurons or in the neurons of the motor facial nucleus (this study; Kloss et al., 1999). Second, α7 is upregulated in the cell bodies of both motor and sensory neurons after injury. In contrast, we see no changes in the levels of α4 expression in DRG neurons after injury as judged either by immunocytochemistry or *in situ* hybridization. These observations show that there are at least three distinct mechanisms by which integrin–ECM interactions can be altered after injury to promote sensory neuron

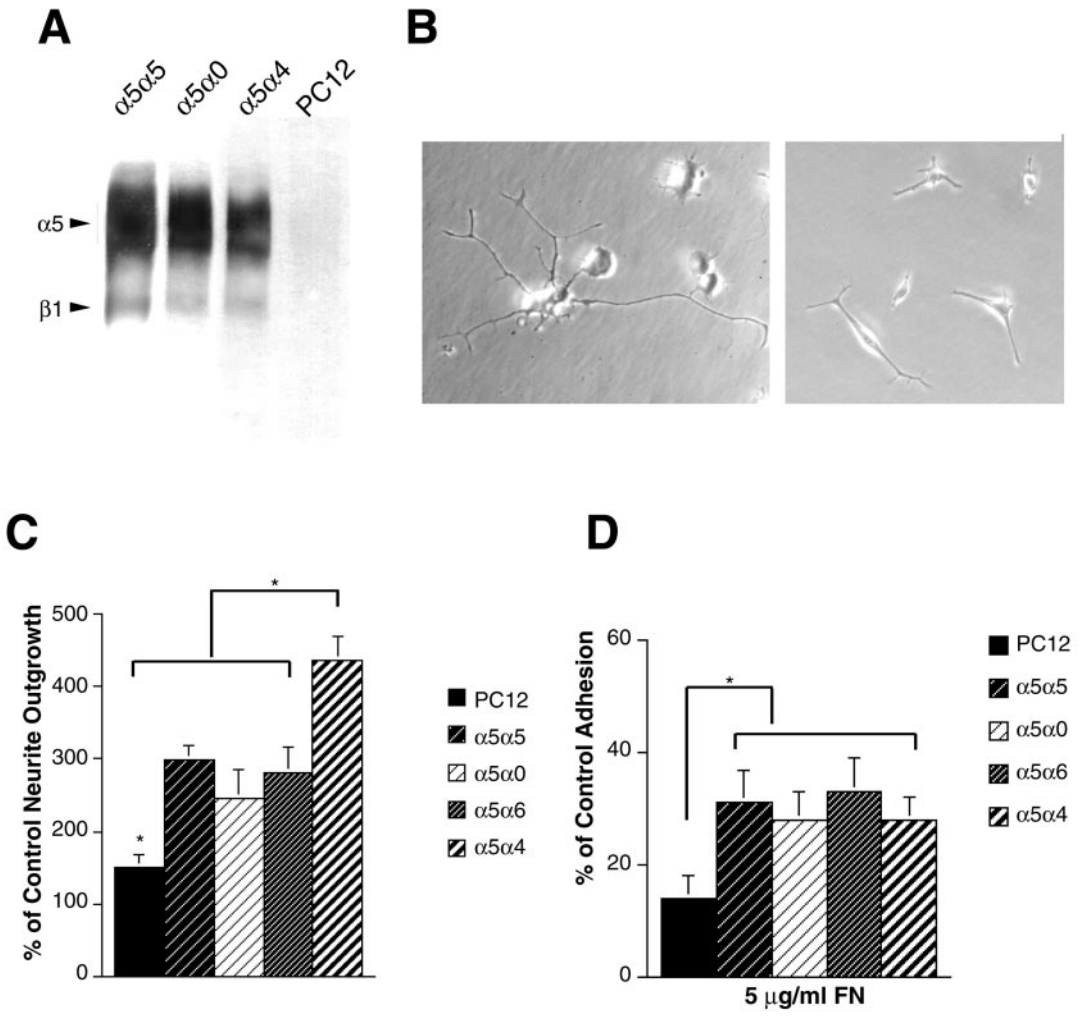

Figure 7. Effect of chimeric α5 integrins on PC12 neurite outgrowth. *A,* PC12 cell lines expressing α5α5, α5α0, and α5α4 chains were surface-labeled with biotin and extracted with 1% Triton X-100. Immunoprecipitations were performed on equal amounts of protein with anti-human α5 antibody and analyzed as by SDS-PAGE on 7% gels followed by detection with streptavidin peroxidase and ECL. Note the similar levels of expression of all chimeras. *B,* Phase micrographs of individual PC12 cells expressing different chimeras and grown on 8V0 substrates. Note the enhanced outgrowth of the α5α4 cell line. *C,* Quantification of the enhanced outgrowth of the α5α4 cells. Cell lines expressing α5α5, α5α0, α5α4, and untransfected PC12 were plated on 8V0, and their neurites were measured after 24 and 48 hr. In each experiment the neurites of at least 50 cells were measured, the median was determined, and the values normalized to PC12 control after 24 hr. Data represent the mean outgrowth at 48 hr of seven separate experiments conducted with three independently generated clonal lines ± SEM. Note the enhanced outgrowth of the α5α4 cell line ($^*p < 0.05$). *D,* Adhesion of α5α5, α5α0, α5α6, α5α4, and mock-transfected cell lines on FN. Adhesion assays were performed as described in Material and Methods. Plates were coated with 50 nM FN fragments. Results are reported as the mean ± SD of three experiments, each performed in quadruplicate. Note that there is no difference between the different α5 cell lines ($^*p < 0.05$).

repair: first, by increasing the levels of ECM proteins, as described for a number of molecules including fibronectin and laminin; second, by upregulation of the integrin receptor as seen with α7; and third, as we show in this study, by alterations in the expression of integrin binding sites within individual ECM molecules as a consequence of alternative splicing. Clearly, these mechanisms are complementary, and this study taken together with that of Lefcort et al. (1992) showing upregulation of FN during peripheral nerve regeneration shows how the first and third mechanisms may operate simultaneously. Importantly, these mechanisms together provide a means to enhance α4-mediated regeneration without any changes being required in the levels of α4 expressed on the growth cones. However, we cannot exclude the possibility that changes in either the level of α4 integrin activation or the subcellular localization, in the absence of any changes in overall expression level, also contribute to enhancing repair.

α4 integrin signaling mechanisms

Our results showing an instructive role for the α4 cytoplasmic domain are consistent with previous studies using chimeric α4 extracellular domain integrins in K562 and Chinese hamster ovary (CHO) cells. The α4 cytoplasmic tail increased cell migration when compared with α2 and α5 tails but reduced cell spreading, diminished adhesion strengthening under conditions of shear flow, and impaired localization of the α4β1 integrin into focal adhesion complexes (Kassner et al., 1995). Enhanced migration with the α4 cytoplasmic domain was also seen in studies using α2 extracellular domain chimeras in rhabdomyosarcoma cells (Chan et al., 1992b). This evidence for increased migration and neurite

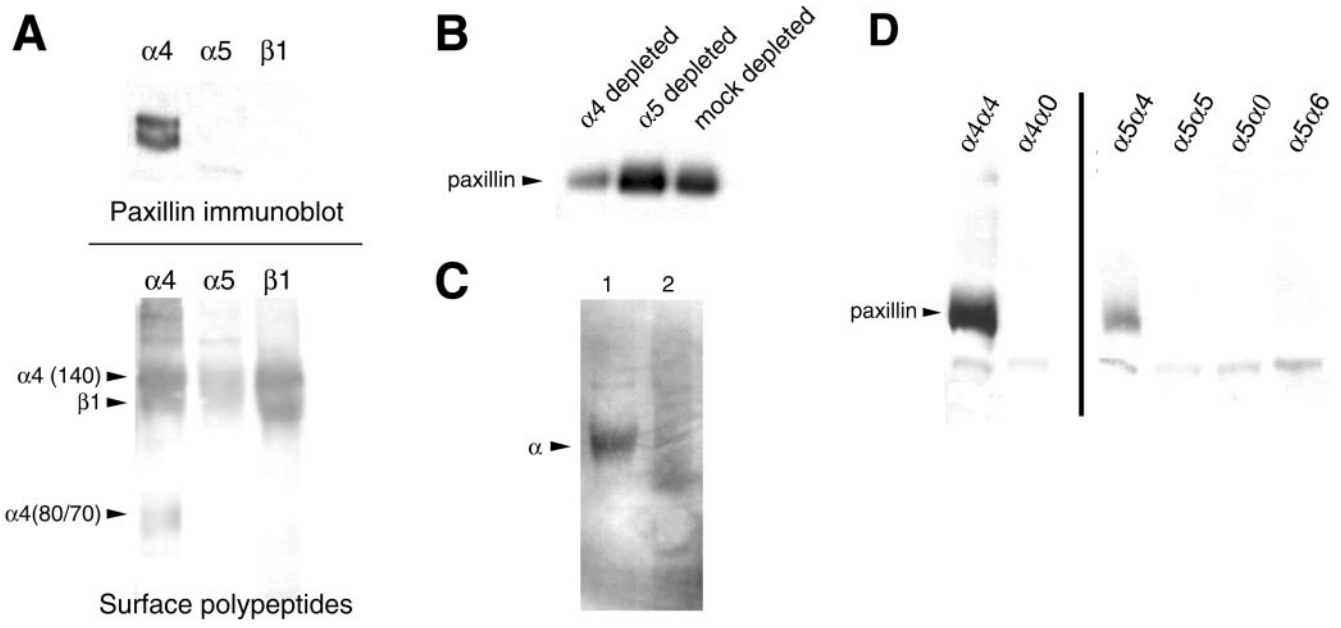

Figure 8. Association of paxillin with the α4 tail. *A,* Identification of paxillin by Western blotting immunoprecipitates generated using anti-α4, but not using anti-β1 or anti-α5, from biotin-labeled lysates of DRG neurons (*top panel*). Two paxillin bands were detected, probably representing the α and β isoforms of paxillin. The presence of immunoprecipitated cell-surface proteins in the material used for Western blotting was confirmed by detection with streptavidin peroxidase and ECL (*bottom panel*). *B,* Immunoprecipitation of paxillin from the DRG neuron lysates after multiple immunodepletions with anti-α4, anti-α5, or irrelevant IgG (α4, α5, mock depletions). Note the reduction in the level of paxillin in the lysate depleted of α4 integrins. *C,* Reimmunoprecipitation of α4 (*lane 1*) but not α5 (*lane 2*) from immunoprecipitates generated using anti-paxillin antibodies on lysates of DRG neurons. *D,* Cell lysates from PC12 cell lines expressing α4α4, α4α0, α5α5, α5α0, α5α6, or α5α4 were immunoprecipitated with anti-human α4 (*lanes 1, 2*) or α5 (*lanes 3–6*) and then Western blotted with anti-paxillin antibodies. Equal amounts of protein were used. Note that only those cell lines expressing the α4 cytoplasmic domain show coassociation of paxillin.

outgrowth suggests that the α4 cytoplasmic domain triggers specific intracellular signaling pathways regulating these complex aspects of cell behavior. A potential mechanism is provided by the recent observation that the α4 cytoplasmic domain binds to the signaling adapter protein paxillin, whereas other α cytoplasmic domains fail to bind. This association increased the rates of focal adhesion kinase phosphorylation and cell migration but reduced cell spreading (Liu et al., 1999; Liu and Ginsberg, 2000). We show here that the α4 cytoplasmic domain also binds paxillin in DRG neurons and PC12 cells. The PC12 cell experiments also showed that the cytoplasmic domain was sufficient for binding, because both α4α4 and α5α4 chimeras co-precipitated with paxillin in detergent extracts. As described in CHO cells, no association with the β1 cytoplasmic domain was present in our study.

This association of α4 and paxillin is interesting because a number of studies implicate paxillin in neurite extension. Paxillin is an adapter protein able to integrate adhesion and growth factor signaling via a number of different binding domains (Turner, 2000). Previous studies have shown changes in paxillin phosphorylation in association with neurite outgrowth. Integrin-mediated adhesion to laminin in neurons stimulates neurite outgrowth and causes both an increase in tyrosine phosphorylation of paxillin and redistribution of tyrosine-phosphorylated paxillin into the cytoskeletal fraction (Leventhal and Feldman, 1996; Curtis and Malanchini, 1997). Tyrosine phosphorylation of paxillin in PC12 cells is stimulated by the neurite outgrowth-promoting nerve growth factor (NGF) (Khan et al., 1995; Escalante et al. 2000). Whereas regulation of tyrosine phosphorylation is recognized as a mechanism controlling growth cone behavior (Bixby and Jhavbala, 1992; Goldberg and Wu, 1996; Desai et al., 1997; Cheng et al., 2000), the mechanistic relationship between paxillin phosphorylation and neurite outgrowth is unclear. Phosphorylation of tyrosines 31 and 118 is necessary for the interaction with the adapter molecule CrkII and collagen-induced cell migration (Petit et al., 2000), and a mutant CrkII (Y222F) prevents NGF-stimulated neurite outgrowth (Escalante et al., 2000). However, expression of a triple tyrosine mutant form of paxillin (Y to F for tyrosines 31, 118 and 187, preventing phosphorylation) had no effect on PC12 neurite outgrowth induced by cooperative collagen and growth factor signaling (Ivankovic-Dikic et al., 2000). An alternative mechanism, unlinked to phosphorylation of these tyrosines, by which paxillin might regulate neurite outgrowth is suggested by a recent study showing that deletion of a highly conserved leucine-rich domain (LD4) reduces neurite outgrowth stimulated by cooperative integrin–growth factor signals (Ivankovic-Dikic et al., 2000). This region of paxillin binds PKL, which links paxillin with a protein complex including PIX, PAK, and Nck (Turner et al., 1999). This complex has been implicated in Rho-family GTPase signaling and could therefore regulate the cytoskeletal interactions associated with growth cone motility and neurite extension.

Although the mechanisms remain unclear, these different studies do show a role for paxillin in neurite extension. We propose, therefore, that the tight association of α4 and paxillin ensures the immediate recruitment of this adapter protein to the adhesion complex, bypassing any need for a diffusion-based mechanism to relocate critical signaling molecules within the membrane (Teruel and Meyer, 2000). The association of α4 with a multidomain adapter protein also provides a mechanism for integrating α4β1 integrin signaling and that from other adhesion receptors. In a recent study using retinal neurons, Treubert and Brummendorf (1998) observed that FN-mediated neurite outgrowth was en-

hanced by the IgSF molecule F11 and that this enhanced outgrowth could not be blocked by RGD peptides. Based on the lack of effect of the RGD peptides, they proposed that the α4β1 integrin might be responsible for a FN-mediated signal that could be amplified by additional interaction of the cell with F11. Our results support such a role for α4β1 and suggest coassociated paxillin as one potential integrator of the FN and F11 signaling pathways.

In conclusion, our results add significantly to our knowledge of the function of FN splicing by providing support for a model in which the increased inclusion of V25 that follows injury in peripheral nerve results in enhanced outgrowth of sensory neurons expressing α4β1 integrin. The splicing pattern of the V25 region in human FN resembles that of the rat and the LDV sequence is conserved. The identification of the α4 cytoplasmic domain and coassociated paxillin as important signaling components therefore suggests these molecules as therapeutic targets for drugs to enhance peripheral nerve repair in humans, and further studies on the molecular signaling complexes associated with these molecules are required.

REFERENCES

Agius E, Cochard P (1998) Comparison of neurite outgrowth induced by intact and injured sciatic nerves: a confocal and functional analysis. J Neurosci 18:328–338.

Bailey S, Eichler M, Villadiego A, Rich K (1993) The influence of fibronectin and laminin during Schwann cell migration and peripheral nerve regeneration through silicon chambers. J Neurocytol 22:176–184.

Bixby J, Jhavbala P (1992) Inhibition of tyrosine phosphorylation potentiates substrate-induced neurite growth. J Neurobiol 23:468–480.

Brezinschek RI, Brezinschek HP, Lazarovits AI, Lipsky PE, Oppenheimer-Marks N (1996) Expression of the beta 7 integrin by human endothelial cells. Am J Pathol 149:1651–1660.

Chan B, Kassner P, Schiro J, Byers H, Kupper T, Hemler M (1992b) Distinct cellular functions mediated by different VLA integrin alpha subunit cytoplasmic domains. Cell 68:1051–1060.

Cheng S, Mao J, Rehder V (2000) Filopodial behavior is dependent on the phosphorylation state of neuronal growth cones. Cell Motil Cytoskel 47:337–350.

Curtis ID, Malanchini B (1997) Integrin-mediated tyrosine phosphorylation and redistribution of paxillin during neuronal adhesion. Exp Cell Res 230:233–243.

Desai CJ, Sun Q, Zinn K (1997) Tyrosine phosphorylation and axon guidance: of mice and flies. Curr Opin Neurobiol 7:70–74.

Dufour S, Duband J-L, Humphries M, Obara M, Yamada K, Thiery J (1988) Attachement, spreading and locomotion of avian neural crest cells are mediated by multiple adhesion sites on fibronectin molecules. EMBO J 7:2661–2671.

Dumoulin FL, Raivich G, Streit WJ, Kreutzberg GW (1991) Differential regulation of calcitonin gene-related peptide (CGRP) in regenerating facial nucleus and dorsal root ganglion. Eur J Neurosci 3:338–342.

Escalante M, Courtney J, Chin W, Teng K, Kim J-I, Fajardo J, Mayer B, Hempstead B, Birge R (2000) Phosphorylation of c-Crk II on the negative regulatory Tyr 222 mediates nerve growth factor-induced cell spreading and morphogenesis. J Biol Chem 275:24787–24797.

ffrench-Constant C (1995) Alternative splicing of fibronectin-Many different proteins, but few different functions. Exp Cell Res 221:261–271.

Goldberg D, Wu D (1996) Tyrosine phosphorylation and protrusive structures of the growth cone. Perspect Dev Neurobiol 4:183–192.

Guan J-L, Hynes R (1990) Lymphoid cells recognize an alternatively spliced segment of fibronectin via the integrin receptor α4β1. Cell 60:53–61.

Gutman A, Kornblihtt A (1987) Identification of a third region of cell-specific alternative splicing in human fibronectin mRNA. Proc Natl Acad Sci USA 84:7179–7182.

Humphries M, Akiyama S, Komoriya A, Olden K, Yamada K (1988) Neurite extension of chicken peripheral neurons on fibronectin: relative importance of specific adhesion sites in the central-binding domain and the alternatively spliced type III connecting segment. J Cell Biol 106:1289–1297.

Ivankovic-Dikic I, Gronroos E, Blaukat A, Barth B-U, Dikic I (2000) Pyk2 and FAK regulate neurite outgrowth induced by growth factors and integrins. Nat Cell Biol 2:574–581.

Kassner P, Alon R, Springer T, Hemler M (1995) Specialized functional properties of the integrin alpha 4 cytoplasmic domain. Mol Biol Cell 6:661–674.

Khan MA, Okumura N, Okada M, Kobayashi S, Nakagawa H (1995) Nerve growth factor stimulates tyrosine phosphorylation of paxillin in PC12h cells. FEBS Lett 362:201–204.; 207.

Kil S, Krull C, Cann G, Clegg D, Bronner-Fraser M (1998) The α4 subunit of integrin is important for neural crest cell migration. Dev Biol 202:29–42.

Kloss, C, Werner A, Klein M, Shen J, Menuz K, Probst J, Kreuzberg G, Raivich G (1999) Integrin family of cell adhesion molecules in the injured brain: regulation and cellular localization in the normal and regenerating mouse facial motor nucleus. J Comp Neurol 411:162–178.

Kloss C, Bohatschek M, Kreutzberg GW, Raivich G (2001) Effect of lipopolysaccharide on the morphology and integrin immunoreactivity of ramified microglia in the mouse brain and in cell culture. Exp Neurol, in press.

Kornblihtt A, Umezawa K, Vibe-Pedersen K, Baralle F (1985) Primary structure of human fibronectin: differential splicing generate at least 10 polypeptides from a single gene. EMBO J 4:1755–1759.

Lefcort F, Venstrom K, McDonald JA, Reichardt LF (1992) Regulation of expression of fibronectin and its receptor, α5β1, during development and regeneration of peripheral nerve. Development 116:767–782.

Leventhal P, Feldman E (1996) Tyrosine phosphorylation and enhanced expression of paxillin during neuronal differentiation *in vitro*. J Biol Chem 271:5957–5960.

Liu S, Ginsberg M (2000) Paxillin binding to a conserved sequence motif in the α4 integrin cytoplasmic domain. J Biol Chem 275:22736–22742.

Liu S, Thomas S, Woodside D, Rose D, Kiosses W, Pfaff M, Ginsberg M (1999) Binding of paxillin to α4 integrins modifies integrin-dependent biological responses. Nature 402:676–681.

Magnuson V, Young M, Schattenberg D, Mancini M, Chen D, Steffensen B, Klebe R (1991) The alternative splicing of fibronectin is altered during aging and in response to growth factors. J Biol Chem 266:14654–14662.

Martini R (1994) Expression and functional roles of neural cell surface molecules and extracellular matrix components during development and regeneration of peripheral nerves. J Neurocytol 23:1–28.

Mathews GA, ffrench-Constant C (1995) Embryonic fibronectins are up-regulated following peripheral nerve injury in rats. J Neurobiol 26:171–188.

Moller JC, Klein MA, Haas S, Jones LL, Kreutzberg GW, Raivich G (1996) Regulation of thrombospondin in the regenerating mouse motor facial nucleus. Glia 17:121–132.

Peters J, Chen G, Hynes R (1996) Fibronectin isoform distribution in the mouse. II. Differential distribution of the alternatively spliced EIIIB, EIIIA, and V segments in the adult mouse. Cell Adhes Commun 4:127–148.

Petit V, Boyer B, Lentz D, Turner C, Thiery J-P, Valles A (2000) Phophorylation of tyrosine residues 31 and 118 on paxillin regulates cell migration through an association with CRK in NBT-II cells. J Cell Biol 148:957–969.

Relvas JB, Setzu A, Baron W, Buttery P, LaFlamme S, Franklin RJM, ffrench-Constant C (2001) Expression of dominant negative and chimeric subunits reveals an essential role for beta 1 integrin during myelination. Curr Biol 11:1039–1043.

Reichardt LF, Tomaselli KJ (1991) Extracellular matrix molecules and their receptors: functions in neural development. Annu Rev Neurosci 14:531–570.

Ruoslahti E (1996) RGD and other recognition sequences for integrins. Annu Rev Cell Dev Biol 12:697–715.

Scherer S, Salzer J (1996) Axon-Schwann cell interactions during peripheral nerve degeneration and regeneration. In: Glial cell development: basic principles and clinical relevance. (Jessen K, Richardson W, eds), pp 165–196. Oxford, UK: BIOS Scientific.

Schwarzbauer J, Tamkun J, Lemischka I, Hynes R (1983) Three different fibronectin mRNA arise by alternative splicing of the rat fibronectin gene transcript. Cell 35:421–431.

Schwarzbauer J, Patel R, Fonda D, Hynes R (1987) Multiple sites of alternative splicing of the rat fibronectin gene transcript. EMBO J 6:2573–2580.

Sheppard A, Onken M, Rosen G, Noakes P, Dean D (1994) Expanding roles for α4 integrin and its ligands in development. Cell Adhes Commun 2:27–43.

Stepp M, Urry L, Hynes R (1994) Expression of alpha 4 mRNA and protein and fibronectin in the early chicken embryo. Cell Adhes Commun 2:359–375.

Tamkun J, Schwarzbauer J, Hynes R (1984) A single rat fibronectin gene generates three different mRNAs by alternative splicing of a complex exon. Proc Natl Acad Sci USA 81:5140–5144.

Teruel MN, Meyer T (2000) Translocation and reversible localization of signaling proteins: a dynamic future for signal transduction Cell 103:181–184.

Tomaselli K, Damsky C, Reichardt L (1987) Interactions of a neuronal cell line (PC12) with laminin, collagen IV, and fibronectin: identification of integrin-related glycoproteins involved in attachment and process outgrowth. J Cell Biol 105:2347–2358.

Tomaselli K, Hall D, Flier L, Gehlsen K, Turner D, Carbonetto S, Reichardt L (1990) A neuronal cell line (PC12) expresses two β1-class

integrins-$\alpha 1\beta 1$ and $\alpha 3\beta 1$-that recognize different neurite outgrowth-promoting domains in laminin. Neuron 5:651–662.
Toyota B, Carbonetto S, David S (1990) A dual laminin/collagen receptor acts in peripheral nerve regeneration. Proc Natl Acad Sci USA 87:1319–1322.
Treubert U, Bruemmendorf T (1998) Functional cooperation of $\beta 1$-integrins and members of the Ig superfamily in neurite outgrowth induction. J Neurosci 18:1795–1805.
Turner C (2000) Paxillin and focal adhesion signalling. Nat Cell Biol 2:E231–236.
Turner C, Brown M, Perrotta J, Riedy M, Nikopoulos S, McDonald A, Bagrodia S, Thomas S, Leventhal P (1999) Paxillin LD4 motif binds PAK and PIX through a novel 95-kD ankyrin repeat, ARF-GAP protein: a role in cytoskeletal remodeling. J Cell Biol 145:851–863.
Vogelezang M, Scherer S, Fawcett J, ffrench-Constant C (1999) Regulation of fibronectin alternative splicing during peripheral nerve repair. J Neurosci Res 56:323–333.
Wagner N, Loehler J, Kunkel E, Ley K, Leung E, Krissansen G, Rajewski K, Mueller W (1996) Critical role for $\beta 7$ integrins in formation of the gut-associated lymphoid tissue. Nature 382:366–370.
Wang GY, Hirai KI, Shimada H, Taji S, Zhong SZ (1992) Behavior of axons, Schwann cells and perineurial cells in nerve regeneration within transplanted nerve grafts - effects of anti-laminin and anti-fibronectin antisera. Brain Res 583:216–226.
Wayner E, Garcia P, Humphries M, McDonald J, Carter W (1989) Identification and characterization of the T lymphocyte adhesion receptor for an alternative cell attachment domain (CS-1) in plasma fibronectin. J Cell Biol 109:1321–1330.
Werner A, Willem M, Jones L, Kreutzberg G, Mayer U, Raivich G (2000) Impaired axonal regeneration in $\alpha 7$ integrin-deficient mice. J Neurosci 20:1822–1830.
Yang JT, Rayburn H, Hynes RO (1995) Cell adhesion events mediated by alpha 4 integrins are essential in placental and cardiac development. Development 121:549–560.
Zardi L, Carnemolla B, Siri A, Petersen T, Paolella G, Sebastio G, Baralle F (1987) Transformed human cells produce a new fibronectin isoform by preferential alternative splicing of a previously unobserved exon. EMBO J 6:2337–2342.
Zhang X, Xu ZO, Shi TJ, Landry M, Holmberg K Ju G, Tong YG, Bao L, Cheng XP, Wiesenfeld-Hallin Z, Lozano A, Dostrovsky J, Hokfelt T (1998) Regulation of expression of galanin and galanin receptors in dorsal root ganglia and spinal cord after axotomy and inflammation. Ann NY Acad Sci 863:402–413.